

## Silicon Nanowire Biosensors for Diabetes Mellitus Monitoring

M. Shaifullah A. Sa<sup>a</sup>, J. Jumath<sup>b</sup>, M. N. M. Nuzaihan<sup>a\*</sup>, M. F. M. Fathila<sup>a</sup>, J. Ismail<sup>a</sup>, N. H. A. Halim<sup>a</sup>, Z. Zailan<sup>b</sup>, M. K. Md Arshad<sup>a,b</sup>, M. Syamsul<sup>c,d</sup>, Rozaimah A. T<sup>e</sup>

<sup>a</sup>Institute of Nano Electronic Engineering, Universiti Malaysia Perlis, 01000 Kangar, Perlis, Malaysia

<sup>b</sup>Faculty of Electronic Engineering & Technology, Universiti Malaysia Perlis, 02600 Arau, Perlis, Malaysia

<sup>c</sup>Institute of Nano Optoelectronics Research and Technology, USM, 11900 Pulau Pinang, Malaysia

<sup>d</sup>Faculty of Science and Engineering, Waseda University, Shinjuku, Tokyo 169-8555, Japan

<sup>e</sup>Bandar Baharu District Health Office, 09800 Serdang, Kedah

\*Corresponding author. Tel.: +6012-4296433; e-mail: m.nuzaihan@unimap.edu.my

Received 22 September 2023, Revised 21 June 2024, Accepted 24 June 2024

### ABSTRACT

The main goal of this research is the development of a label-free biosensor for the detection of diabetes mellitus (DM) using the target molecule retinol-binding protein 4 (RBP4). The enzyme-linked immunosorbent assay (ELISA) approach, currently used to detect DM, is time-consuming and difficult. As a result, label-free biosensors are being considered as an alternative. In this research, silicon nanowires (SiNWs) were selected as the transducer for this biosensor due to their low cost, real-time analysis capability, high sensitivity, and low detection limit. The SiNWs were created using conventional lithography, reactive ion etching (RIE), and physical vapor deposition (PVD), and then dripped with a gold nanoparticle solution to create gold-decorated SiNWs. The surface of the gold-decorated SiNWs was functionalized using 3-aminothiophenol and glutaraldehyde solutions before being immobilized with DM RBP4 antibodies and targets. The electrical characterization of the gold nanoparticle decorated SiNWs biosensor revealed good performance in DM detection. The pH tests confirmed that the SiNWs acted as a transducer, with current proportional to the DM RBP4 concentration. The estimated limit of detection (LOD) and sensitivity for detecting DM RBP4 binding were 0.076 fg/mL and 8.92 nA(g/mL)<sup>-1</sup>, respectively. This gold nanoparticle decorated SiNWs biosensor performed better than other methods and enabled efficient, accurate, and direct detection of DM. The SiNWs could be used as a distinctive electrical protein biosensor for biological diagnostic purposes. In conclusion, gold nanoparticle deposition offers effective label-free, direct, and high-accuracy DM detection, outperforming previous approaches. Thus, these SiNWs serve as novel electrical protein biosensors for future biological diagnostic applications.

**Keywords:** Silicon nanowire, Diabetes mellitus, Retinol Binding Protein 4, Electrical detection

### 1. INTRODUCTION

In recent years, diabetes mellitus (DM) has emerged as a pressing global health concern. The condition affects millions of individuals worldwide, with over 86 million adults [1] experiencing elevated blood sugar levels, often progressing from type 1 to type 2 diabetes. This alarming trend is not confined to any particular region; it affects both developed and developing nations, propelled by contemporary lifestyles, economic growth, and urbanization. The consequences of diabetes are profound, impacting individuals on physical, social, and financial levels. Diabetes, characterized by chronically elevated blood glucose levels [2], results from a deficiency in insulin production or impaired cellular response to insulin. Consequently, diabetic patients experience increased blood glucose levels, which can have serious health implications if not managed effectively. Late diagnosis of sugar imbalances can lead to severe complications such as stroke or renal failure. Multiple factors, including lifestyle choices, weight, and genetics, contribute to the development of diabetes, which is categorized into three types: type 1, type 2, and gestational diabetes [2]. Traditional diagnostic approaches

for diabetes monitoring have limitations, including labour-intensive procedures, the need for substantial sample volumes, lengthy analysis times, and complex detection systems [1]. Biosensors have emerged as a cutting-edge solution for measuring glucose concentration to address these challenges. Biosensors utilize specific biochemical reactions mediated by bioreceptors to detect chemical compounds, offering a versatile and advanced detection method. Recent developments in biosensor technology have enhanced stability, sensitivity, selectivity, shelf life, reusability, miniaturization, and cost-effectiveness [3].

One promising biomolecule of interest in diabetes research is retinol-binding protein 4 (RBP4), which has demonstrated potential as a novel adipokine implicated in insulin resistance and the development of type 2 diabetes. Studies in animals and humans have shown associations between elevated RBP4 levels and insulin resistance, highlighting its significance in diabetes pathogenesis [4]. Moreover, research has shown a growing interest in label-free detection methods for various analytes, including proteins and viruses, using field-effect transistors (FET) or chemo-resistive sensors. These sensors offer high

sensitivity and selectivity without the need for fluorescent or chemical tags. Nanotechnology has played a pivotal role in advancing biosensors, with materials such as nanoparticles, graphene quantum dots, and electrospun nanofibers enhancing biosensor design and functionality [4]. These nanomaterials have significantly improved biosensors' affinity, selectivity, and efficacy in detecting target molecules. Among nanomaterials, silicon nanowire field-effect transistors (SiNW FETs) have garnered significant attention. SiNW FETs, characterized by their remarkable electronic properties, small dimensions, and real-time label-free detection capabilities, are particularly promising for biosensing applications. The project at hand utilizes SiNWs to implement nanotechnology in biosensors. SiNWs offer potential solutions for developing miniaturized, cost-effective biosensors that are compatible with traditional silicon technology. Due to their large surface-to-volume ratio, nanowires enable efficient interactions with biological molecules, significantly changing electrical conductivity [5]. As a result, SiNW biosensors are expected to provide exceptional sensitivity.

In summary, the escalating prevalence of DM and the limitations of traditional monitoring methods have led to significant advancements in biosensor technology, particularly SiNW biosensors. These biosensors hold promise for real-time glucose monitoring and other applications in diabetes management, offering patients more convenient and effective tools for maintaining their blood glucose levels within a healthy range.

DM is a long-term metabolic condition that primarily manifests as insulin resistance or insufficiency. Those with diabetes will have several problems, including issues with the microvascular and macrovascular systems (coronary artery disease and peripheral arterial disease). Patients with DM also experience additional side effects such as osteoporosis, an elevated risk of fractures, inadequate fracture healing, periodontal disease, gingivitis, diabetic myonecrosis, trigger finger, frozen shoulder, and rotator cuff tendinopathy [6]. Every diabetic complication incurs costs for both the patient and society. Direct and indirect costs impact families, friends, and public health programs [6]. DM comes in various forms. Type 1 diabetes mellitus (T1DM) is a chronic autoimmune disease characterized by a high blood glucose level due to a lack of insulin. The primary cause of insulin insufficiency is the immune cell invasion and attack on  $\beta$ -cells, leading to their destruction.  $\beta$ -cells in the pancreas produce insulin, a crucial hormone that facilitates glucose absorption in other organs. Uncontrolled blood sugar can lead to complications such as microalbuminuria, neuropathy, and microvascular diseases. In one study of young Malaysians with T1DM [7], 52 diabetics between the ages of 12 and 20 were identified.

The major features of type 2 diabetes mellitus (T2DM) are insulin resistance and insufficient or inadequate insulin production. Poor glucose tolerance or fasting glycemia increases the likelihood of developing type 2 diabetes. Additionally, modern dietary patterns and rising environmental pollution contribute to the increasing prevalence of T2DM [8]. T2DM accounts for over 90% of all cases of adult-onset DM in Malaysia, making it the most

common type [9]. It places a heavy socioeconomic burden on society due to earlier death and higher morbidity caused by accelerated vascular issues [10]. Gestational diabetes mellitus (GDM) is a common pregnancy issue found in women without a history of type 1 or type 2 diabetes during the second or third trimester [11]. According to Xie et al., [11] GDM has been linked to an increased risk of severe perinatal outcomes, such as spontaneous abortion, pregnancy-induced hypertension, eclampsia, dystocia, postpartum hemorrhage, an increased cesarean section rate, premature birth, and macrosomia. A history of GDM increases a person's chance of developing type 2 diabetes mellitus by up to eight times. Children exposed to GDM are more likely to become obese and have cardiovascular illnesses as adults [12]. RBP4 is a lipocalin protein that transports retinol (vitamin A) in the blood. Recent research indicates that overweight mice and people frequently have higher blood levels of RBP4, making the body less responsive to insulin [13].

Conventional diagnostic methods for diabetes have limitations, including complexity and time consumption. Biosensors, on the other hand, are emerging as advanced tools for glucose monitoring. These devices have evolved significantly, offering benefits such as sensitivity, selectivity, miniaturization, and cost-effectiveness. Biosensors utilize biochemical reactions mediated by receptors to detect specific molecules, with RBP4 being a potential biomolecule of interest. Nanotechnology has played a significant role in enhancing biosensors. Nanomaterials like nanoparticles, graphene quantum dots, and electrospun nanofibers have improved biosensor performance. In particular, SiNWs have gained attention for their potential in biosensors. SiNWs offer advantages such as real-time label-free detection, remarkable electronic properties, and compatibility with traditional silicon technology. They have a high surface-to-volume ratio, enabling precise interactions with biological substances and resulting in highly sensitive biosensors. Combining biosensors and nanotechnology, specifically SiNW, holds promise for developing miniature, cost-effective biosensors capable of real-time analysis and early detection of diabetes and other health conditions. The term "biosensor" refers to a device that uses specific biochemical responses mediated by bioreceptors, such as immune systems, isolated enzymes, organelles, tissues, or whole cells, to detect chemical molecules, often using thermal, electrical, or optical signals [14]. The goal and layout of the biosensor affect analyte detection. Several everyday objects, like smartphones, can be used as biosensors with the right accessories. For instance, Castillo-Henriquez et al. [15] developed a non-invasive, saliva-based smartphone biosensor for urea, enabling quick, low-cost preliminary detection. The second element of a biosensor system is the transducer, also referred to as a detector. A transducer converts physicochemical changes at the bioreceptor (such as intensity, temperature, light, pH, and conductivity) through a process known as "signalization" into a different type of energy signal [16]. The final element of the biosensor is the reading device section. Many intricate electronic components are used in biosensor systems to digitize, amplify, filter, and multiplex electronic signals in order to provide a result [15-17].

Nanowires are nanostructures with a one-dimensional morphology characterized by significant aspect ratios of length to diameter. These structures have special properties, including unique electrical conductivity, mechanical strength, thermal behaviour, and optical response. The fabrication of nanowires can be achieved by top-down or bottom-up methods, depending on their specific characteristics, including shape and material composition. Barbosa et al. [17] have reported that many biomolecules, such as enzymes, antibodies, and nucleic acids, can be easily modified for use on nanowires. Similarly, a nanomaterial's formation and physical characteristics depend upon its method of fabrication and manufacture. The top-down technique involves the reduction of large quantities of material into nanoparticles, whereas the bottom-up method entails the opposite process of synthesizing nanoparticles from smaller components [18]. Nanomaterials are formed by atom and molecule growth and self-assembly, creating nanostructures with distinct forms, sizes, and chemical compositions. SiNWs exhibit considerable potential in the advancement of miniaturized, cost-effective biosensors within the realm of silicon technology. These biosensors are capable of real-time analysis of diverse bacterial strains, offering higher sensitivity and a minimal detection limit [19]. The attractiveness of nanowires lies in their extensive contact surface area, characterized by a high surface-to-volume ratio. This property facilitates significant interactions with immobilized biological entities, leading to substantial alterations in electrical conduction via the network of SiNWs [19]. The operational areas commonly observed in field-effect transistor biosensors are the off-state, subthreshold, and saturation regions. The SiNW biosensor demonstrated its maximum sensitivity in the subthreshold range. Various techniques can be employed to enhance a biosensor's threshold voltage, such as channel doping and manipulation of its working mechanism [20].

Nanoparticles have recently been recognized as the most advanced in scientific research and commercial applications. Fullerenes, including polymeric nanoparticles, ceramic nanoparticles, and metal nanoparticles, exemplify nanoparticles that exhibit noteworthy physiological and biological attributes. Due to their diminutive dimensions at the nanoscale level and expansive surface area, nanoparticles exhibit distinctive chemical and physico-chemical properties. The utilization of nanoparticles for surface functionalization presents a promising approach for manipulating cellular and extracellular processes in diverse biological contexts. This method holds potential for various applications, including enzyme inhibition, transport facilitation, sensing capabilities, and transcription regulation [21]. The utilization of this method is important in a wide range of technological and biological research applications. Surface modification of SiNW biosensors is essential for enhancing their ability to detect biomolecules such as Deoxyribonucleic Acid (DNA), Ribonucleic Acid (RNA), enzymes, cells, antibodies, and proteins. Numerous studies have investigated various surface functionalization methods to improve the selectivity and sensitivity of SiNW biosensors [22]. SiNW FET-based sensors have been used for detecting various biomolecular interactions, including protein-protein interactions, oligonucleotide hybridization,

immunodetection, and protein-ligand binding. Surface functionalization can be categorized into two main components: surface modification and immobilization. Surface modification techniques are employed to alter the surfaces of materials in nano-biodesives. Various approaches can be utilized for this purpose, including the application of self-assembled layers, the creation of surface chemical gradients, the initiation of surface chemical processes, and the incorporation of surface-active bulk additives. Self-assembled monolayers (SAMs) are the most highly organized structures that can be formed on particular substrates after chemical surface modification. In addition to surface modification, the technique of surface immobilization is also crucial for a wide range of biosensing applications. Two predominant approaches exist for immobilizing biomolecules onto surfaces, namely covalent and non-covalent techniques. Non-covalent immobilization approaches, such as physical adsorption, are characterized by simplicity and speed. However, it is important to note that these techniques lead to the formation of arrays of immobilized biomolecules that lack well-defined characteristics and exhibit increased instability. Covalent immobilization techniques, such as silane chemistry and SAM, provide a more stable means of immobilization. SAMs are created through molecules with specified functional groups adsorbing spontaneously onto a surface. On the other hand, silanization refers to the attachment of biomolecules to a surface using silane chemistry. According to the study conducted by Barbosa et al. [17], the deposition of gold nanoparticles has been found to boost the surface area, facilitate a large dynamic range, and exhibit exceptional electrical behaviour.

The primary determinant in using SiNW for detection lies in measuring the change in electrical properties resulting from variations in the number of positive or negative charges present on the surface of the nanowires. The phenomenon of the gate effect observed in SiNW can be attributed to the fluctuation in current levels resulting from the interaction between charged target molecules and the nanowire surface. According to Meir et al. [23], binding charged target molecules to SiNWs can result in an accumulation or depletion of charge carriers within the SiNWs [24]. The increase and decrease of electrical charge are determined by the properties of the SiNW (specifically, whether they are N-type doped or P-type doped) and the charge of the target molecules (whether they are positive or negative). The categorization of SiNW is mostly based on the presence of charge carriers. Specifically, SiNW that exhibits an abundance of positively charged electron holes is referred to as p-type doped SiNW. When a biomolecule with a positive charge attaches to p-type SiNW, these electron holes form, reducing conductance and current. Conversely, binding a biomolecule with a negative charge to p-type SiNW will enhance the conductance and current. In contrast, in n-type doped SiNW, where most of the carriers are negatively charged electrons, the binding of negatively charged biomolecules leads to a reduction in conductance and current. Conversely, the binding of positively charged biomolecules increases conductance and current [24]. Recent developments in nanotechnology have made integrating nanoparticles into biodiagnostics a distinct possibility. A wide variety of biomaterials, including

chitosan, collagen, metal nanoparticles, graphene, carbon-based nanomaterials, silicon nanomaterials, dendrimers, and quantum dots, have been used to develop numerous biosensing devices. Rhodium, silver, palladium, platinum, and gold metal nanoparticles are used in physical and chemical processes because they involve less substrate and resources [25]. One of the most important factors affecting the use of nanomaterials and their applications in various fields is the synthesis and growth process of nanostructures and nanomaterials. A nanostructured material might be a great choice for one application, but if created using a different procedure and strategy, it might be more beneficial in another. Gold nanoparticles are among the many nanoparticles frequently used in biosensors; their surface functionalization, extraordinary chemical stability, biorecognition, and signal amplification properties are the primary reasons for their high demand in biotechnology [26]. Gold nanoparticles are among the highest biocompatible nanoparticle systems and have grown popular [27].

Lastly, adding gold nanoparticles to biosensors improves their ability to capture analytes while lowering LOD [28]. The findings from the fabrication of SiNW utilizing RIE and traditional photolithography for contact pads are covered in the following section. To confirm the device's operation, two characterization processes, physical and electrical, were carried out during the manufacture of SiNW. One of the most commonly used gold fabrication techniques is deposition. Techniques that can be used to attach or deposit nanomaterials on electrodes include electrospinning, electrochemical deposition, laser scribing, inkjet printing, and drop casting [29]. The drop-casting deposition technique was employed in this study to deposit gold nanoparticles and carry out surface modification, immobilization, and protein binding. Drop casting was chosen because of its benefits, affordability, usability, and relatively low precipitation temperature [30]. Drop casting is preferred in this study because it has advantages in small-area deposition and can be used to fabricate SiNW devices at the nanoscale. According to a recent study, drop casting is becoming increasingly popular among researchers due to its outstanding crystal structure, which improves device performance. A certain quantity of solution is first made and then poured on top of the substrate. The substrate is then allowed to evaporate for a predetermined amount of time. Research suggests baking the device on a hotplate to improve evaporation. On top of the substrate, a thin solid coating will develop when the solution has dried.

The analytical performance of SiNW biosensors is crucial in determining their efficacy in detecting and measuring diverse biological analytes. SiNWs have been shown to exhibit great sensitivity, selectivity, and a low detection limit, making them appropriate for a wide range of biosensing applications. SiNW biosensors have been the subject of extensive research due to their high sensitivity and potential for ultrasensitive detection of biomolecules. They utilize the unique properties of nanomaterials (in this research, their electronic properties) to enable sensitive detection. When comparing various input target concentrations, a biosensor with high sensitivity produces an output *ID* difference with a greater value, making

interpretation simpler. The sensitivity of the biosensor, defined as the ratio of the changes in current to the changes in analyte concentration, is expressed in Equation (1).

$$\text{Sensitivity} = \Delta \text{Current} / \Delta \text{Analyte concentration} \quad (1)$$

Equation (1) reported by [31] aims to detect low-concentration analytes, particularly in complex biological matrices, where heightened sensitivity is required. The Limit of Detection (LOD) is a crucial analytical parameter that determines the lowest concentration of an analyte consistently identifiable and quantifiable using a particular analytical procedure. LOD helps provide recent biosensor findings to advance biomolecule technology [32]. Determining LOD is important to ensure the accuracy and reliability of the method [33]. Improving the LOD limit ensures that the technology application keeps advancing and consequently contributes to various scientific domains.

To the best of our knowledge, the development of SiNW for the detection of DM has been largely unexplored so far. Due to the potential and important applications of the biosensor in diagnosing large populations suffering from DF, we report herein, for the first time, the use of gold nanoparticle decorated SiNWs biosensor for DM monitoring. Adding gold nanoparticles to biosensors improves their ability to capture analytes, lowers the LOD, boosts the surface area, facilitates a large dynamic range, and exhibits exceptional electrical behavior. In other words, we expect this research to be the best solution for resolving the addressed issues, promising the realization of electrical biosensors in the development of the next generation of electrical biosensors used in hospitals and for the commercialization of devices.

## 2. METHODS

The method and fabrication procedure for gold nanoparticle decorated SiNWs are described in this section. The process flow for creating gold nanoparticle-decorated SiNWs is depicted in a flowchart in Figure 1.

### 2.1. Fabrication of gold nanoparticle decorated SiNWs

In this research, silicon wafers were utilized as samples, and AutoCAD was used to create the mask for the nanowire pattern. Preparing the sample is the first stage of fabrication. The silicon wafer was cut into 2cm × 2cm dimensions after being cleaned and prepared for sample preparation. Following cleaning, the wafer went through the traditional photolithography process. The primary goal of the photolithography technique is to use ultraviolet (UV) light to transfer a geometric pattern from a mask to the surface of a photoresist/silicon wafer. Photolithography involves several stages, including photoresist coating, soft baking, mask alignment, exposure and development, and hard baking. In this research, positive photoresists were applied to the whole silicon wafer surface following coating. The sample must be gently baked to remove the solvent and harden the film. After that, ultraviolet (UV) radiation transfers the chrome mask's design to the sample's surface. Due to the positive photoresist used, the exposed area of the photoresist is soluble, and the developer develops the soluble area. If the photoresist on the sample did not

overdevelop, the pattern of the SiNW is examined using a high-power microscope (HPM) after the development process, and the hard baking procedure is employed to increase the adhesion of the resist to the sample surface. Following a specified RIE recipe setup, the sample is put through RIE to etch the silicon before proceeding with contact pad deposition using PVD. Following that, an HPM analysis of the sample's surface morphology was taken. The SiNW was dripped with a gold nanoparticle solution to create gold nanoparticle decorated SiNWs. Finally, an electrical measurement of the SiNW with decorations was made. The process flow is shown in Figure 2.

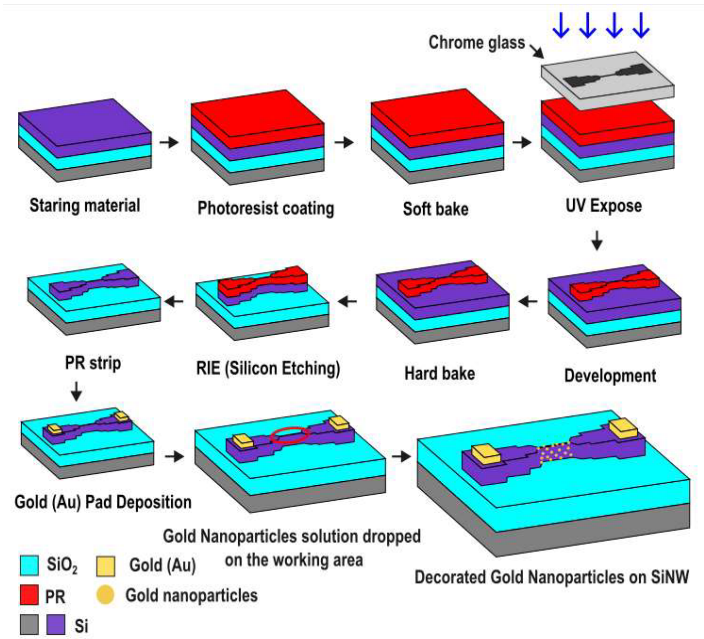


Figure 2. The process flow for the fabrication of gold nanoparticle decorated SiNWs.

## 2.2. Surface functionalization technique

Functionalization of the SiNW surface with bio-recognition elements is a crucial step in constructing a biosensor, enabling the device to detect a specific target molecule and providing a robust set of tools for this purpose. Surface modification, surface immobilization, and protein binding are the three stages involved in this functionalization, as shown in Figure 3. 3-aminothiophenol solution and Glutaraldehyde (GA) solution (2.5%) were used in the surface modification process. These two solutions play an important role in the formation of self-assembly monolayers and provide cross-link capability. First, the device was cleaned using Deionized (DI) water to remove any impurities or contamination on the surface. The 3-aminothiophenol solution was diluted using DI water. 0.5µl of 3-aminothiophenol solution was dropped onto the gold nanoparticle decorated SiNWs. To form a SAM, the device was kept at room temperature for 12 hours. Then, the device was cleaned using DI water several times to remove any unbound or excess 3-aminothiophenol molecules. Electrical characterization techniques were again performed to examine the current – voltage (I-V) curve of the device. Next, 10µl of glutaraldehyde (GA) was dropped onto the SiNW, where 2.5% of the GA was diluted with phosphate-buffered saline (PBS). Glutaraldehyde acts as a linking agent to activate the amino ends of 3-aminothiophenol molecules on the SiNWs. The device was air-dried in a dark environment to ensure the effectiveness of the GA activation. After the activation step, the device was rinsed with DI water and air-dried at room temperature. Finally, the I-V curve of the device was examined.

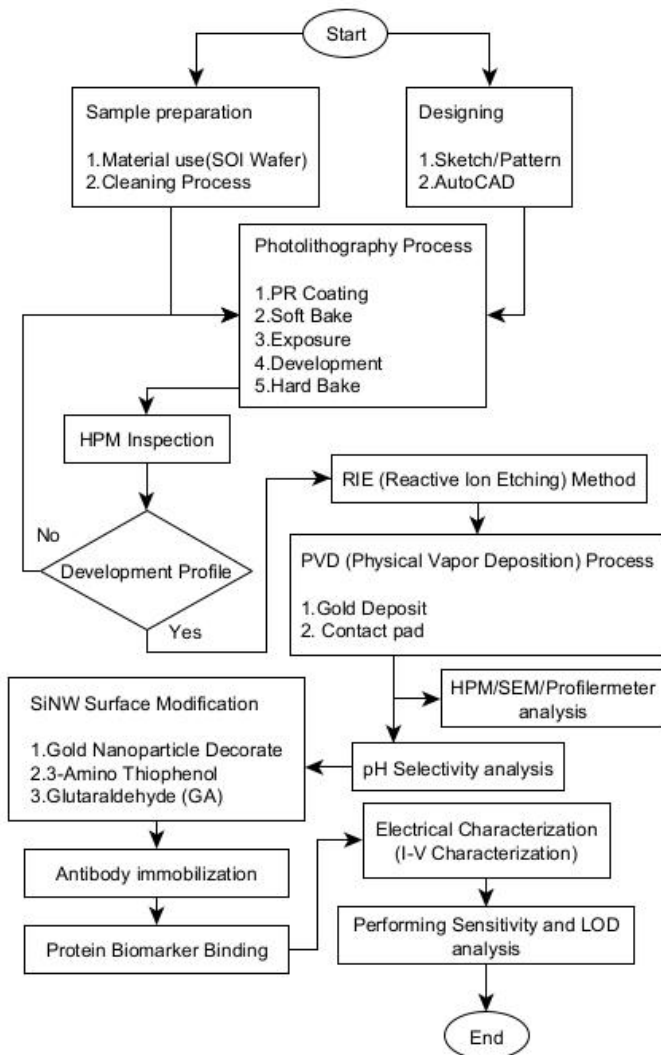


Figure 1. The overall flowchart for the fabrication of gold nanoparticle decorated SiNWs.



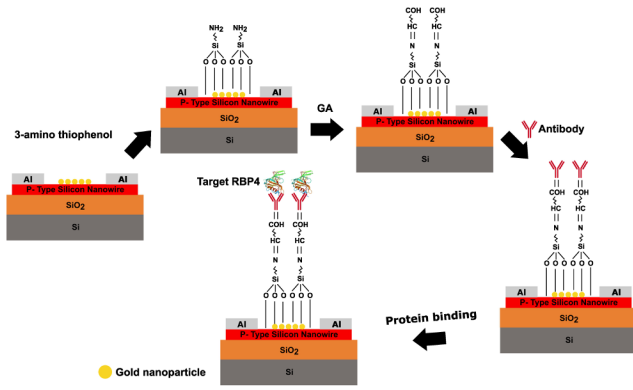


Figure 3. The surface functionalization of SiNW.

### 2.3. Surface immobilization and protein binding

The RBP4 antibody solution was prepared at a concentration of  $1\mu\text{g/ml}$ , where the RBP4 was diluted with  $10\text{mM}$  PBS.  $10\mu\text{l}$  of the solution was dropped onto the dried glutaraldehyde on the device. The sample was then dried at room temperature for 6 hours to adhere to the surface and form a stable attachment. Electrical characterization for this step was performed after the RBP4 antibody solution was completely dried. Then, the device was immersed in  $0.1\%$  Bovine Serum Albumin (BSA) for a few minutes to avoid nonspecific binding. Since the only available BSA in the lab had a concentration of  $10\%$ , the solution was diluted with  $20\mu\text{l}$  of  $0.01\text{M}$  PBS. The device was then washed with DI water several times and dried. After the device was dried, its I-V curve was analyzed before storing it at a temperature of  $4^\circ\text{C}$ . This ensured the stability of the immobilized antibodies. In protein binding, three concentrations of the targeted RBP4 were analyzed:  $0.02\text{ pg/mL}$ ,  $0.05\text{ pg/mL}$ , and  $0.40\text{ pg/mL}$ . Each concentration was dropped onto the SiNW using the drop-casting method and left at room temperature until the solution dried (estimated time around 6 hours), and the I-V curve of the device was examined after it had dried.

## 3. RESULTS AND DISCUSSION

### 3.1. Morphological characterization of SiNW

Figure 4 shows the normal developmental pattern structure of nanowires with its cross-section at A-A' under HPM. Based on Figure 4, the color of the SOI was turquoise, while the resist was red. There were some tiny dots of resist on its SOI surface; however, this resist will not cause any short to the nanowires since it is not connected to either the source or drain of the device. The next outcome is the underdeveloped pattern structure of the nanowire [34]. In this outcome, most of the surface part of the SOI wafer is still covered with resist, and the pattern of the device could not be distinguished. Figure 5 shows the nanowire's underdeveloped pattern structure with its cross-section at A-A'. As shown in Figure 5, the entire wafer surface was still covered with resist since the whole surface is in red color. The only difference that can be observed is the shade of red; the desired pattern had a darker red color while everything around was in a brighter red color. Another characteristic

that can be observed is that the nanowires are still connected from the drain to the source [34].

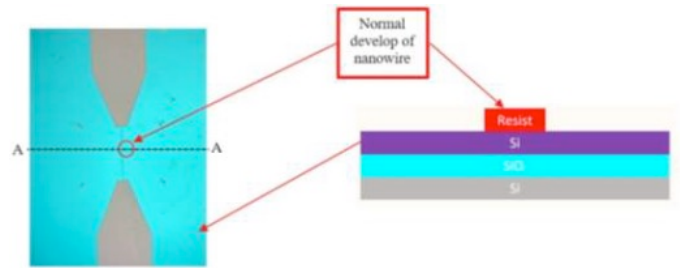


Figure 4. Normal development pattern structure of nanowire with its cross-section at A-A'.

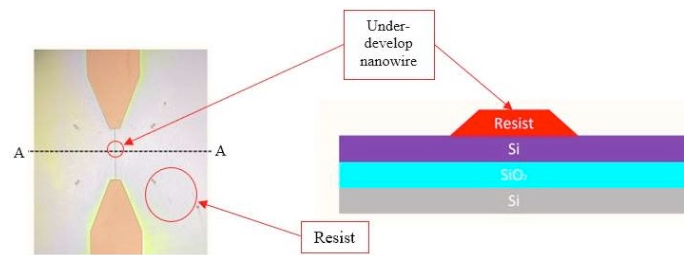


Figure 5. Under-develop pattern structure of nanowire with its cross-section at A-A'.

The last profile is the over-developed pattern structure of the nanowire [34]. This outcome usually relates to disconnected wires, where the nanowire is not connected from drain to source. Figure 6 shows the over-developed pattern structure of the nanowire with its cross-section at A-A'.

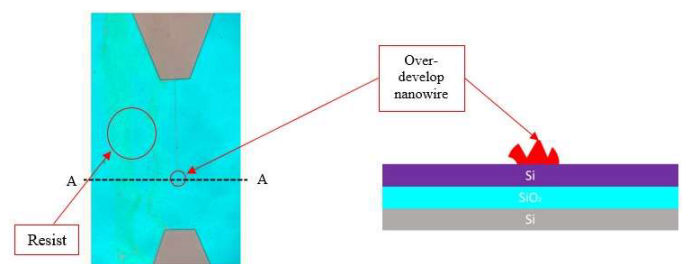
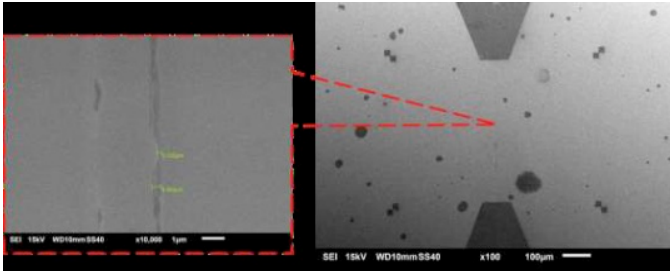


Figure 6. Over-develop pattern structure of nanowire with its cross section at A-A'.

Based on Figure 6, the observation that can be made is that the nanowire is no longer connected from source to drain, indicating that the wire was over-etched [34]. Despite the nanowire being overly etched, there was still resist spotted outside the nanowire device. The resist outside the targeted pattern outline was connected from the drain to the source. This condition occurs due to human error since the development process was conducted by humans. Errors such as uneven development of the resist developer cause this condition to occur.

After the conventional lithography process was completed, the sample underwent the RIE process to reduce the width of the wires. The initial wire width is 1  $\mu\text{m}$ , and after the RIE process, the final wire width is approximately 200 nm. The wire width was reduced by 800 nm through the RIE process, making this device in the nano scale. From Figure 7, at x100 magnification, the SiNW was barely visible, thus the magnification of the scanning electron microscopy (SEM) was increased to x10,000. At 10,000 magnification, the minimum and maximum wire widths were selected. The width measurements for its minimum and maximum values were 200 nm.



**Figure 7.** The SEM image of 200 nm wide SiNW s at x100 magnification with an inset of SiNW at x10,000 magnification.

Other than SEM, the device was also observed using a profilometer. In the profilometer, two measurements were generated: depth and width, as shown in Figure 8. In Figure 8 (a), the minimum depth selected was  $-0.8774 \text{ \AA}$ , where 1  $\text{Å}$  is equivalent to 0.1 nm. In the optical profilometer, minimum and maximum are selected manually.  $-0.8774 \text{ \AA}$  is selected as the minimum depth value since the value is close to one. The maximum height was  $291.499 \text{ \AA}$ , selected at the peak of the graph. In nanometers, the minimum and maximum depth values were  $-0.08774 \text{ nm}$  and  $29.14991 \text{ nm}$ , respectively. Delta is the change of variable; the delta value can be confirmed by using the formula highest value minus lowest value. Therefore,  $\Delta$  depth [ $-0.08774 \text{ nm} - (29.14991 \text{ nm})$ ] is  $29.23765 \text{ nm}$ . Figure 8 (b) shows the width of the SiNW. The starting position for SiNW width, when the graph point starts to increase rapidly, is seen at line R. The value at point R is  $34.5328 \mu\text{m}$ . The second position in width is when the graph point decreases rapidly, which is shown at line M, where M is equal to  $36.1017 \mu\text{m}$ . The delta value for width can be confirmed by subtracting the value of position M from the value of position R. Therefore,  $\Delta$  width is approximately 200 nm. In this study, both SEM and optical profilometer were used to measure the surface topography of SiNW. However, SEM is an advanced technique for surface topography evaluation; therefore, both techniques generate two different values. Referring to Figures 7 and 8(b), the width values collected for SEM and optical profilometer were approximately 200 nm. This occurs due to the optical profilometer's limitation in resolution, making the technique unable to provide accurate values when evaluating small nanowires.

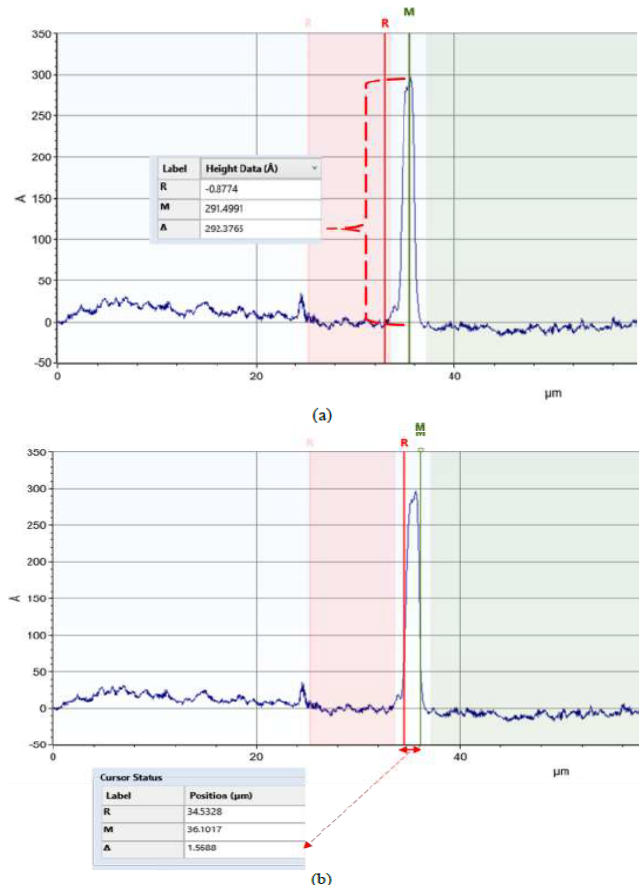


**Figure 8.** (a) The profilometer image for SiNWs height. (b) the profilometer image for SiNWs width.

### 3.2. Electrical characterization

Electrical SiNW biosensor characterization has been achieved for pH sensors and DM RBP4 protein detection. The pH value experiment was electrically characterized to determine the device's functionality by using direct current (DC) voltage that was swept from 0 V to 2 V (a short voltage range). Figure 9 shows the measurement setup of the fabricated SiNW biosensor. All these measurements were made at ambient temperature (room temperature). Changes in electrical current determine the operation of the device. For each measurement, a 0.5  $\mu\text{L}$  droplet of two different pH solutions was applied to the SiNW surface to accomplish the pH electrical characterizations. Figure 10 shows a graph of drain-source current ( $I_{\text{ds}}$ ) versus drain-source voltage ( $V_{\text{ds}}$ ) that illustrates the electrical response to various pH levels. The device displays a good output of the electrical characteristic  $I_{\text{ds}}$  versus  $V_{\text{ds}}$ , indicating an almost linear relationship (ohmic behavior) [35]. The instrument displays the same curve trend behavior, with bare + DI water at the top and bare + pH 7 and bare below; the graph shows DI water has a higher pH value than pH 7. The measured current for bare at 1.0 V of  $V_{\text{ds}}$  is 0.03316 A, for bare + pH 7, it is 0.04202 A, and for bare + DI water, it is 0.04433 A.

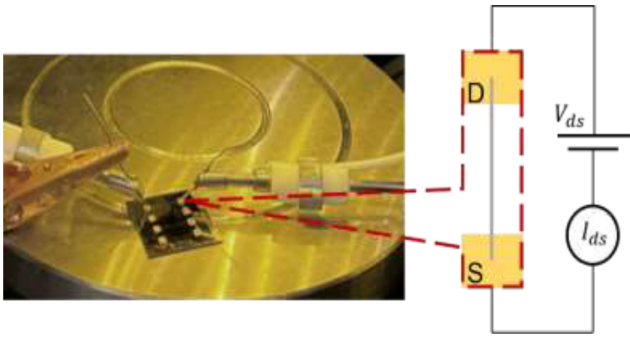


**Figure 9.** The measurement setup of the SiNW biosensor.

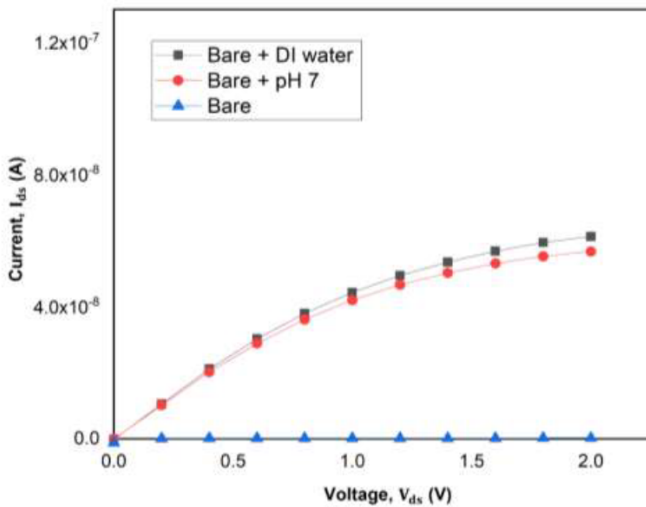


**Figure 10.**  $I_{ds}$ - $V_{ds}$  characteristic of SiNW with the bare condition and several drops of DI water and pH 7.

Figure 10 demonstrates that the current rises as pH values increase. This pattern is consistent with an experimental study of the SiNW FET sensor's impact on pH sensitivity previously published by Gasparyan et al. [36], which found that the  $I_{ds}$  in a solution medium is inversely proportional to the pH level. The reduction in SiNW resistance, which was 30.157 M $\Omega$  for bare, 23.789 M $\Omega$  for bare + pH 7, and 22.558 M $\Omega$  for bare + DI water at 1.0 V, respectively, led to a rise in current. The discovery that SiNWs with high current have low resistance is consistent with Ohm's law. In this study, the detection of DM RBP4 is performed using SiNW biosensors decorated with gold nanoparticles at various protein-binding concentrations. The device is first bound to three distinct protein concentrations (0.02 pg/mL, 0.05 pg/mL, and 0.40 pg/mL) before being electrically tested to determine its I-V characteristics. Figure 11 displays a plot of the interaction's  $V_{ds}$  versus  $I_{ds}$  for various protein concentrations. The outcome is then analyzed in relation to how various protein concentrations impact the I-V curve graph. Observations show that the curve follows a similar pattern as protein concentration increases. The  $I_{ds}$  of 0.40 pg/mL protein concentration exhibit the maximum value when a  $V_{ds}$  of 2.0 V is applied, followed by 0.05 pg/mL and 0.02 pg/mL protein concentration.

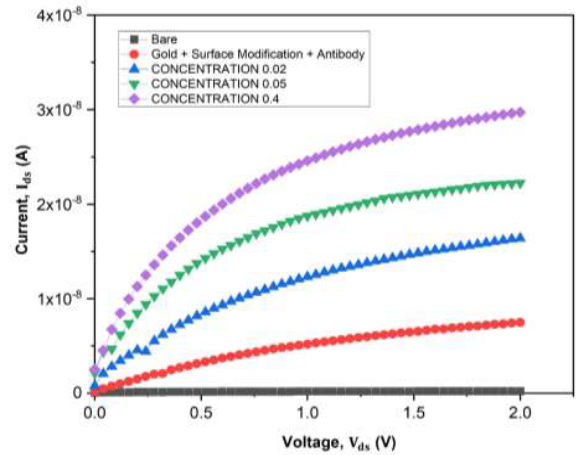


**Figure 11.**  $I_{ds}$ - $V_{ds}$  characteristic of gold nanoparticle decorated SiNW for DM RBP4 using concentrations of 0.02, 0.05, and 0.40 (pg/mL).

The measured current for protein concentration 0.02 pg/mL, 0.05 pg/mL, and 0.40 pg/mL were 0.02458 A, 0.01874 A, and 0.01232 A, respectively, at 1.0 V of  $V_{ds}$ . This pattern is consistent with earlier findings from gold-nanorod improved dielectric voltammetry detection in Letchumanan et al. [37], which revealed that current flow increased as protein content increased. Resistance was 81.16883 M $\Omega$ , 53.36179 M $\Omega$ , and 40.68348 M $\Omega$  at 1.0 V for concentrations of 0.02, 0.05, and 0.40 pg/mL, respectively. This demonstrates a decreasing trend in the resistance of SiNW, which eventually caused an increase in current. Additionally, as the current density increases, the electrical conductance values of p-type SiNW rise due to the accumulation of extra holes brought about by binding negatively charged protein concentrations to their surface [37]. Consequently, it can be said that larger protein concentrations result in more holes building up in the SiNWs, enhancing the device's conductivity [37]. The increased conductance results in a higher current flow across the SiNWs, demonstrating that the SiNW sensor was responsive to observable chemical modifications and reactions. This tendency is supported by a related trend finding by another researcher [38], who found that high protein concentrations result in high electron-hole densities, thereby increasing current conductivity.

### 3.3. Sensitivity of the gold nanoparticle decorated SiNW

To demonstrate the sensitivity of the SiNW biosensor, the effects of varying concentrations of DM RBP4 target at 0.02 pg/mL, 0.05 pg/mL, and 0.40 pg/mL at  $V_{ds} = 1.0$  V were examined. The ratio between the relative change in the current percentage and the difference in the target DM RBP4 concentration served as a measure of the device's sensitivity. Figure 12 demonstrates that  $I_{ds}$  is proportional to the desired DM RBP4 concentration. The  $I_{ds}$  value increased with the rise in target concentration. More negative charge on the surface of a charged particle causes a build-up of charge carriers (holes) along the perimeter of a p-type SiNW, increasing the observed  $I_{ds}$  [39]. According to the calibration curve, the biosensor has a linear detection and a sensitivity of 8.92 nA(g/mL)<sup>-1</sup>.



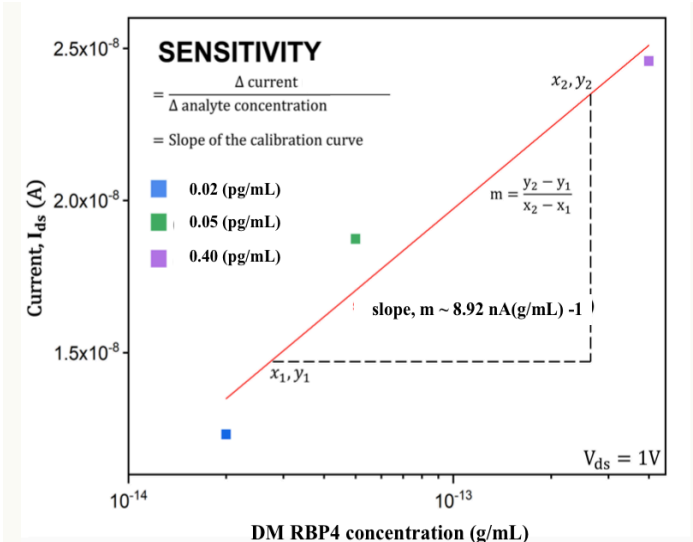


**Figure 12.**  $I_{ds}$  response curve of gold nanoparticle decorated SiNW biosensor with different concentrations of DM RBP4.

### 3.4. LOD for the SiNWs biosensor

In addition to sensitivity, the LOD, which can be used to determine the lowest concentration of an analyte, should also be fully considered. Similar to sensitivity, LOD is demonstrated by the effects of varying DM RBP4 target concentrations at 0.02 pg/mL, 0.05 pg/mL, and 0.40 pg/mL at  $V_{ds} = 1.0$  V. After calculating the device's change in relative current in response to the target concentration of DM RBP4, a linear calibration curve (10 against DM RBP4 concentration) was displayed in Figure 13. The correlation coefficient ( $R^2 = 0.9787$ ) and the estimated LOD is around 0.076 fg/mL.

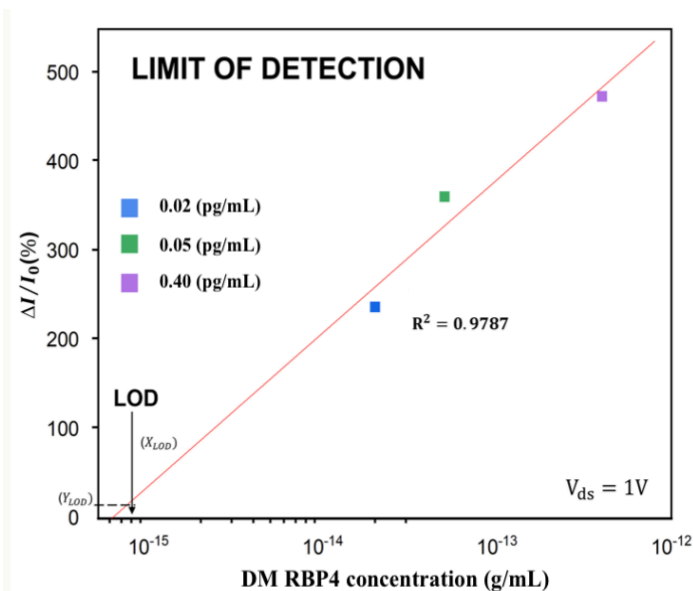


**Figure 13.** LOD of the gold nanoparticle decorated SiNW biosensor.

## 4. CONCLUSION

The invention and manufacturing of the SiNW biosensor with gold nanoparticle deposition resulted in several positive outcomes, including the ability to detect the target

DM RBP4 at various concentrations. The top-down method was used to fabricate the gold nanoparticle decorated SiNW SiNW biosensor. Conventional photolithography was employed to transfer the design from the mask onto the wafer surface. RIE was utilized to reduce the size of SiNW from micro to nanoscale, and PVD was used to create contact pads on the source and drain of the electrode. The morphology of the SiNW was characterized using an optical profilometer, HPM, and SEM. The width of the SiNW, which is 200 nm, was measured using an optical profilometer and SEM, respectively. The effectiveness of the SiNW was assessed using DI water and pH 7 solution. The I-V curve demonstrates that  $I_{ds}$  rises as pH increases. The biosensor has a sensitivity of  $8.92 \text{ nA}/(\text{g}/\text{mL})^{-1}$  and an estimated LOD of 0.076 fg/mL, respectively. In conclusion, this biosensor has important implications for healthcare facilities and can potentially be employed as a diagnostic platform for DM.

## ACKNOWLEDGMENTS

I would like to acknowledge the Fundamental Research Grant Scheme (FRGS) support under grant number FRGS/1/2020/STG01/UNIMAP/02/1) from the Ministry of Higher Education, Malaysia. The authors also would like to acknowledge all the team members in INEE and, FKTEN, UniMAP for their guidance and help related to this study.

## REFERENCES

- [1] D. Vigneswari, N. K. Kumar, V. Ganesh Raj, A. Guban, and S. R. Vikash, "Machine Learning Tree Classifiers in Predicting Diabetes Mellitus," *2019 5th Int. Conf. Adv. Comput. Commun. Syst. ICACCS 2019*, no. June, pp.84–87,2019,doi: 10.1109/ICACCS.2019.8728388.
- [2] B. Paul and B. Karn, "ANFIS based Diabetes Mellitus Prediction," *2021 IEEE 8th Uttar Pradesh Sect. Int. Conf. Electr. Electron. Comput. Eng. UPCON 2021*, pp. 1–6,2021,doi: 10.1109/UPCON52273.2021.9667582.
- [3] K. Singh *et al.*, "Optical biosensors for diabetes management: Advancing into stimuli-responsive sensing mechanisms," *Smart Mater. Med.*, vol. 4, no. June2022,pp.91–101,2023,doi: 10.1016/j.smaim.2022.08.003.
- [4] C. Jin *et al.*, "Plasma retinol-binding protein 4 in the first and second trimester and risk of gestational diabetes mellitus in Chinese women: A nested case-control study," *Nutr. Metab.*, vol. 17, no. 1, pp. 1–7, 2020, doi: 10.1186/s12986-019-0425-9.
- [5] M. W. Shun, M. F. Mohamad Fathil, M. K. Md Arshad, M. N. Md Nor, R. A. Rahim, and S. C. B. Gopinath, "The impact of high-k dielectric layers for SiNW-FET biosensor performance improvement," *2019 IEEE Int. Conf. Sensors Nanotechnology, SENSORS NANO 2019*,pp.1–4,2019,doi: 10.1109/SENSORSNANO44414.2019.8940073.
- [6] S. S. K. Reddy and M. H. Tan, *Diabetes mellitus and its many complications*. Elsevier Inc., 2020. doi: 10.1016/B978-0-12-820605-8.00001-2.
- [7] M. N. Nurhanani, M. Hasni, G. A. Mahfuz, and A. Masita, "An Updated Review of Type 1 Diabetes in Malaysia," *IJUM Med. J. Malaysia*, vol. 21, no. 3, pp.

- 15–24, 2022.
- [8] M. Wang, M. Chen, R. Guo, Y. Ding, H. Zhang, and Y. He, "The improvement of sulfuraphane in type 2 diabetes mellitus (T2DM) and related complications: A review," *Trends Food Sci. Technol.*, vol. 129, pp. 397–407, Nov. 2022, doi: 10.1016/j.tifs.2022.10.007.
- [9] MOH, "Malaysia Clinical Practice Guidelines Management Of Type 2 Diabetes Mellitus Quick Reference Guide for Healthcare Professionals," *Clin. Pract. Guidel. Manag. Type 2 Diabetes Mellit.*, 2020, [Online]. Available: [https://www.moh.gov.my/moh/resources/Penerbitan/CPG/Endocrine/QR\\_T2DM\\_6th\\_Edition\\_QR\\_Guide\\_Digital.pdf](https://www.moh.gov.my/moh/resources/Penerbitan/CPG/Endocrine/QR_T2DM_6th_Edition_QR_Guide_Digital.pdf)
- [10] M. of H. M. A. of M. M. M. E. & M. S. F. M. S. A. of M. D. Malaysia, "Clinical Practice Guideline-MANAGEMENT OF TYPE 2 DIABETES MELLITUS, 2020," *Clin. Pract. Guidel.*, no. Sixth edition, 2020.
- [11] J. XIE, L. LI, and H. XING, "Metabolomics in gestational diabetes mellitus: A review," *Clin. Chim. Acta*, vol. 539, pp. 134–143, Jan. 2023, doi: 10.1016/j.cca.2022.12.005.
- [12] K. K. Venkatesh *et al.*, "Trends in gestational diabetes mellitus among nulliparous pregnant individuals with singleton live births in the United States between 2011 to 2019: an age-period-cohort analysis," *Am. J. Obstet. Gynecol. MFM*, vol. 5, no. 1, p. 100785, Jan. 2023, doi: 10.1016/j.ajogmf.2022.100785.
- [13] J. Y. Li, X. X. Chen, X. H. Lu, C. B. Zhang, Q. P. Shi, and L. Feng, "Elevated RBP4 plasma levels were associated with diabetic retinopathy in type 2 diabetes," *Biosci. Rep.*, vol. 38, no. 5, pp. 4–11, 2018, doi: 10.1042/BSR20181100.
- [14] E. R. Kim, C. Joe, R. J. Mitchell, and M. B. Gu, "Biosensors for healthcare: current and future perspectives," *Trends Biotechnol.*, vol. 41, no. 3, pp. 374–395, Mar. 2023, doi: 10.1016/j.tibtech.2022.12.005.
- [15] L. Castillo-Henríquez, M. Brenes-Acuña, A. Castro-Rojas, R. Cordero-Salmerón, M. Lopretti-Correa, and J. R. Vega-Baudrit, "Biosensors for the detection of bacterial and viral clinical pathogens," *Sensors (Switzerland)*, vol. 20, no. 23, pp. 1–26, 2020, doi: 10.3390/s20236926.
- [16] J. R. Aggas and A. Guiseppi-Elie, "Responsive Polymers in the Fabrication of Enzyme-Based Biosensors," *Biomater. Sci. An Introd. to Mater. Med.*, pp. 1267–1286, Jan. 2020, doi: 10.1016/B978-0-12-816137-1.00079-9.
- [17] A. I. Barbosa, R. Rebelo, R. L. Reis, M. Bhattacharya, and V. M. Correlo, "Current nanotechnology advances in diagnostic biosensors," *Med. Devices Sensors*, vol. 4, no. 1, pp. 1–38, 2021, doi: 10.1002/mds3.10156.
- [18] N. Abid *et al.*, "Synthesis of nanomaterials using various top-down and bottom-up approaches, influencing factors, advantages, and disadvantages: A review," *Adv. Colloid Interface Sci.*, vol. 300, p. 102597, Feb. 2022, doi: 10.1016/j.cis.2021.102597.
- [19] Z. Lu *et al.*, "Rapid and quantitative detection of tear MMP-9 for dry eye patients using a novel silicon nanowire-based biosensor," *Biosens. Bioelectron.*, vol. 214, p. 114498, Oct. 2022, doi: 10.1016/j.bios.2022.114498.
- [20] J. Hu *et al.*, "Influence Of B Ions Doping on the Performance of P-Type Silicon Nanowire Field Effect Transistor Biosensor," *2022 China Semicond. Technol. Int. Conf. CSTIC 2022*, vol. 2, no. d, pp. 1–3, 2022, doi: 10.1109/CSTIC55103.2022.9856887.
- [21] F. Ahmad *et al.*, "Unique Properties of Surface-Functionalized Nanoparticles for Bio-Application: Functionalization Mechanisms and Importance in Application," *Nanomaterials*, vol. 12, no. 8, 2022, doi: 10.3390/nano12081333.
- [22] X. Yang, Y. Fan, Z. Wu, and C. Liu, "A Silicon Nanowire Array Biosensor Fabricated by Complementary Metal Oxide Semiconductor Technique for Highly Sensitive and Selective Detection of Serum Carcinoembryonic Antigen," *Micromachines*, vol. 10, no. 11, 2019, doi: 10.3390/mi10110764.
- [23] R. Meir *et al.*, "Direct Detection of Uranyl in Urine by Dissociation from Aptamer-Modified Nanosensor Arrays," *Anal. Chem.*, vol. 92, no. 18, pp. 12528–12537, Sep. 2020, doi: 10.1021/acs.analchem.0c02387.
- [24] H. Li, S. Wang, X. Li, C. Cheng, X. Shen, and T. Wang, "Dual-Channel Detection of Breast Cancer Biomarkers CA15-3 and CEA in Human Serum Using Dialysis-Silicon Nanowire Field Effect Transistor," *Int. J. Nanomedicine*, vol. 17, no. December, pp. 6289–6299, 2022, doi: 10.2147/IJN.S391234.
- [25] M. Hegde, P. Pai, M. G. Shetty, and K. S. Babitha, "Gold nanoparticle based biosensors for rapid pathogen detection: A review," *Environ. Nanotechnology, Monit. Manag.*, vol. 18, p. 100756, 2022, doi: <https://doi.org/10.1016/j.enmm.2022.100756>.
- [26] Y. Gupta and A. S. Ghrrera, "Recent advances in gold nanoparticle-based lateral flow immunoassay for the detection of bacterial infection," *Arch. Microbiol.*, vol. 203, no. 7, pp. 3767–3784, 2021, doi: 10.1007/s00203-021-02357-9.
- [27] D. Franco *et al.*, "Bio-hybrid gold nanoparticles as SERS probe for rapid bacteria cell identification," *Spectrochim. Acta Part A Mol. Biomol. Spectrosc.*, vol. 224, p. 117394, 2020, doi: <https://doi.org/10.1016/j.saa.2019.117394>.
- [28] I. A. Quintela, B. G. De Los Reyes, C. S. Lin, and V. C. H. Wu, "Simultaneous colorimetric detection of a variety of Salmonella spp. In food and environmental samples by optical biosensing using oligonucleotide-gold nanoparticles," *Front. Microbiol.*, vol. 10, no. MAY, pp. 1–12, 2019, doi: 10.3389/fmicb.2019.01138.
- [29] Rodiawan, S. C. Wang, and Suhdi, "Gold-nanoparticle-decorated Tin Oxide of a Gas Sensor Material for Detecting Low Concentrations of Hydrogen Sulfide," *Sensors Mater.*, vol. 35, no. 3, pp. 1121–1130, 2023, doi: 10.18494/SAM4237.
- [30] S. F. madlul, N. K. Mahan, E. M. Ali, and A. N. Abd, "Synthesis of CdS:Cu5% thin films by chemical method based on silicon for gas sensor applications," *Mater. Today Proc.*, vol. 45, pp. 5800–5803, 2021, doi: <https://doi.org/10.1016/j.matpr.2021.03.170>.

- [31] A. Sena-Torralba, R. Álvarez-Diduk, C. Parolo, A. Piper, and A. Merkoçi, "Toward Next Generation Lateral Flow Assays: Integration of Nanomaterials," *Chem. Rev.*, vol. 122, no. 18, pp. 14881–14910, Sep. 2022, doi: 10.1021/acs.chemrev.1c01012.
- [32] S. N. Yusoh and K. A. Yaacob, "Study on the physical properties of a SiNW biosensor to the sensitivity of DNA detection," *Materials (Basel)*, vol. 14, no. 19, 2021, doi: 10.3390/ma14195716.
- [33] A. Barazandeh, G. D. Najafpour, A. Alihosseini, S. Kazemi, and E. Akhondi, "Spectrophotometric determination of naproxen using chitosan capped silver nanoparticles in pharmaceutical formulation," *Int. J. Eng. Trans. A Basics*, vol. 34, no. 7, pp. 1576–1585, 2021, doi: 10.5829/IJE.2021.34.07A.03.
- [34] H. Xiao, "Go To 13.3.2 Local Oxidation of Silicon Page," *Introd. to Semicond. Manuf. Technol. (2nd Ed.)*, Dec. 2012, Accessed: Jul. 24, 2022.
- [35] D. Wang, Y. Liang, Y. Su, Q. Shang, and C. Zhang, "Sensitivity enhancement of cloth-based closed bipolar electrochemiluminescence glucose sensor via electrode decoration with chitosan/multi-walled carbon nanotubes/graphene quantum dots-gold nanoparticles," *Biosens. Bioelectron.*, vol. 130, pp. 55–64, Apr. 2019, doi: 10.1016/J.BIOS.2019.01.027.
- [36] Gasparyan, F., Zadorozhnyi, I., Khondkaryan, H., Arakelyan, A., & Vitusevich, S. (2018). Photoconductivity, pH Sensitivity, Noise, and Channel Length Effects in Si Nanowire FET Sensors. *Nanoscale Research Letters*, 13. <https://doi.org/10.1186/s11671-018-2494-5>
- [37] I. Letchumanan, M. K. Md Arshad, S. R. Balakrishnan, and S. C. B. Gopinath, "Gold-nanorod enhances dielectric voltammetry detection of c-reactive protein: A predictive strategy for cardiac failure," *Biosens. Bioelectron.*, vol. 130, pp. 40–47, 2019, doi: <https://doi.org/10.1016/j.bios.2019.01.042>.
- [38] N. R. Dalila, M. K. M. Arshad, S. C. B. Gopinath, M. N. M. Nuzaihan, and M. F. M. Fathil, "Molybdenum disulfide—gold nanoparticle nanocomposite in field-effect transistor back-gate for enhanced C-reactive protein detection," *Microchim. Acta*, vol. 187, no. 11, p. 588, 2020, doi: 10.1007/s00604-020-04562-7.
- [39] N. Elfström and J. Linnros, "Sensitivity of silicon nanowires in biosensor applications," *J. Phys. Conf. Ser.*, vol. 100, no. 5, p. 052042, Mar. 2008, doi: 10.1088/1742- 6596/100/5/052042.